ACS Pharmacology & Translational Science

pubs.acs.org/ptsci

Article

Identification of Novel UGT1A1 Variants Including UGT1A1 454C>A through the Genotyping of Healthy Participants of the HPTN 077 Study

Herana Kamal Seneviratne, Allyson N. Hamlin, Sue Li, Beatriz Grinsztejn, Halima Dawood, Albert Y. Liu, Irene Kuo, Mina C. Hosseinipour, Ravindre Panchia, Leslie Cottle, Gordon Chau, Adeola Adeyeye, Alex R. Rinehart, Marybeth McCauley, Joseph S. Eron, Myron S. Cohen, Raphael J. Landovitz, Craig W. Hendrix, and Namandjé N. Bumpus*

Cite This: *ACS Pharmacol. Transl. Sci.* 2021, 4, 226–239

Read Online

ACCESS | Metrics & More | Article Recommendations

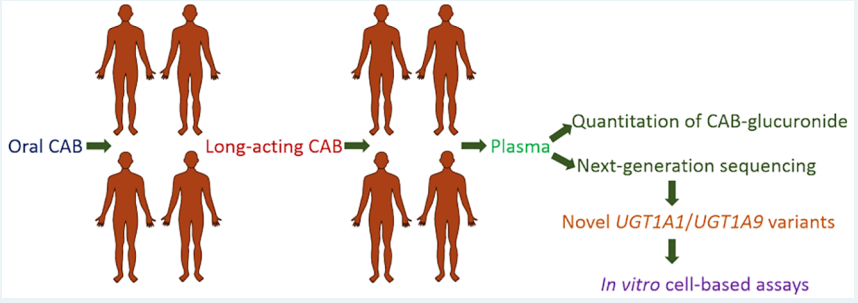

ABSTRACT: Cabotegravir (CAB) is an integrase strand-transfer inhibitor of HIV that has proven effective for HIV treatment and prevention in a long-acting injectable formulation, typically preceded by an oral formulation lead-in phase. Previous *in vitro* studies have demonstrated that CAB is primarily metabolized via glucuronidation by uridine diphosphate glucuronosyltransferase (UGT) 1A1 and 1A9. In this study, we performed next-generation sequencing of genomic DNA isolated from the HPTN 077 participants to explore the variants within *UGT1A1* and *UGT1A9*. Additionally, to enable correlation of *UGT1A1* and *UGT1A9* genotypes with plasma CAB-glucuronide levels, we quantified glucuronidated CAB following both oral administration of CAB and intramuscular injection of long-acting CAB. From these studies, 48 previously unreported variants of *UGT1A1* and *UGT1A9* were detected. Notably, 5/68 individuals carried a *UGT1A1 454C>A* variant that resulted in amino acid substitution P152T, and the use of *in silico* tools predicted a deleterious effect of the P152T substitution. Thus, the impact of this mutant on a range of UGT1A1 substrates was tested using a COS-7 cell-based assay. The glucuronide conjugates of CAB, dolutegravir, and raltegravir, were not formed in the COS-7 cells expressing the UGT1A1 P152T mutant. Further, formation of glucuronides of raloxifene and 7-ethyl-10-hydroxycamptothecin were reduced in the cells expressing the UGT1A1 P152T mutant. Using the same approach, we tested the activities of two UGT1A9 mutants, UGT1A9 H217Y and UGT1A9 R464G, and found that these mutations were tolerated and decreased function, respectively. These data provide insight into previously unreported genetic variants of *UGT1A1* and *UGT1A9*.

KEYWORDS: *cabotegravir, long-acting, human immunodeficiency virus, pre-exposure prophylaxis, uridine diphosphate glucuronosyltransferase, cabotegravir-glucuronide*

Cabotegravir (CAB) is an integrase strand-transfer inhibitor of HIV that has demonstrated efficacy when used alone for HIV pre-exposure prophylaxis (PrEP) and, in combination with rilpivirine, for HIV treatment.[1,2] Of note, CAB is formulated both as an oral tablet and as a long-acting injectable.[3] Long-acting injectable formulations are advantageous in that they do not require daily dosing and thus may lower the barriers to adherence as compared to oral regimens. The acceptability of long-acting injectable agents in PrEP among potential user groups has been reported.[4,5]

As a carbamoylpyridine, CAB contains amide functionality as well as a nitrogen-containing heterocycle.[1] It is structurally similar to dolutegravir, another integrase strand transfer

Received: October 27, 2020
Published: January 21, 2021

inhibitor approved by the FDA in 2013 for HIV treatment.[1,6,7] The antiviral activity of CAB has been demonstrated against a variety of HIV clades and studies using *in vitro* assays have shown that CAB inhibits integrase-catalyzed viral DNA strand transfer with low or subnanomolar efficacy.[8,9] Further, both the aqueous solubility (0.015 mg/mL in pH 6.8 phosphate buffer at 20 °C) and long elimination half-life of CAB favored its development as a long-acting formulation.[8,10] Importantly, CAB also has a relatively high genetic barrier to resistance.[11] The utility of long-acting CAB as a PrEP agent has been evaluated in the context of preventing simian-HIV (SHIV) infection in macaques.[12,13] These preclinical studies demonstrated a high level of protection against repeated intrarectal as well as intravaginal SHIV challenges.[12,13] To date, there have been two Phase IIa clinical studies to evaluate the potential of CAB long-acting as an agent for HIV-1 prevention in humans: ECLAIR and HIV Prevention Trials Network (HPTN) 077.[14,15] The tolerability of long-acting CAB was demonstrated in the HPTN 077 study.[15]

Glucuronidated CAB has been previously identified as the primary metabolite of CAB in humans, mice, rats, and monkeys following oral, subcutaneous, or intramuscular administration.[10] Further, in the above-mentioned work, glucuronidated CAB was the predominant CAB component recovered in urine for each route of delivery. Drug metabolism plays a crucial role in the clearance of drugs from the body.[16] Orally administered drugs often undergo hepatic metabolism, and the liver contains a high abundance of drug metabolizing enzymes including uridine diphosphate glucuronosyltransferases (UGTs).[16,17] UGTs carry out glucuronidation, which is the transfer of glucuronic acid from uridine 5′-diphosphoglucuronic acid to drugs containing amine, carboxylic acid, hydroxyl, phenol, or thiol groups.[17,18] The resulting glucuronide conjugates are more polar than the parent drugs, and these glucuronide conjugates are excreted renally or via biliary elimination.[18] However, since injected drugs enter circulation directly, the potential impact of metabolism on injected drugs often remains unconsidered. Further, for injected drugs that are known to undergo metabolism, it is difficult to ascertain which organs are responsible for the metabolism. Interestingly, CAB has been previously shown to undergo glucuronidation *in vitro* in human kidney microsomes.[19] Reaction phenotyping studies by Bowers et al. have demonstrated that CAB is primarily metabolized by UGT family members UGT1A1 and UGT1A9 with a fractional contribution of 0.67 and 0.33, respectively.[10] Notably, these two enzymes are known to be expressed in a range of extrahepatic tissues, including kidney and intestine.[20,21]

In the present study, we performed next-generation targeted sequencing of genomic DNA isolated from plasma samples collected from HPTN 077 study participants to investigate the presence of variants of *UGT1A1* and *UGT1A9*. We then performed analyses to look for relationships between the *UGT1A1* and *UGT1A9* genotypes and CAB glucuronidation. HPTN 077 was a double-blind, placebo-controlled phase IIa study that evaluated the safety, tolerability, and pharmacokinetics of long-acting CAB in HIV-uninfected individuals.[15] Previously, it was reported that CAB was well tolerated in HPTN 077 participants across study sites in South Africa, Brazil, Malawi, and the United States.[15] In HPTN 077, a 4-week oral phase was followed by an injection phase. For CAB-glucuronide measurements, we obtained samples collected 1 week after the last oral dose of the oral lead-in phase and throughout the injection phase. In this study, we detected 48 previously unreported variants of *UGT1A1* and *UGT1A9*. Of note, 5/68 individuals carried a *UGT1A1* variant that resulted in amino acid substitution P152T, and the use of *in silico* tools predicted a deleterious effect of the P152T substitution. We confirmed this prediction using a cell-based metabolism assay. Taken together, the findings from this study provide insights into genetic variants of *UGT1A1* and *UGT1A9* that may impact the metabolism of CAB and other UGT1A1 and UGT1A9 substrates.

METHODS

Chemicals and Reagents. CAB, dolutegravir (DTG), raltegravir (RAL), raloxifene (RXF), CAB-glucuronide, RAL-glucuronide, and RXF-glucuronide standards were obtained from Toronto Research Chemicals, Inc. (North York, ON, Canada) while 7-ethyl-10-hydroxycamptothecin (SN-38) was obtained from MilliporeSigma (St. Louis, MO). The purities of CAB-glucuronide, RAL-glucuronide, and RXF-glucuronide standards were 95%. All solvents used were high-performance liquid chromatography (HPLC) grade and purchased from Fisher Scientific (Hampton, NH), unless otherwise specified.

Plasma Samples. The HPTN 077 study (ClinicalTrials.gov Identifier: NCT02178800) was carried out as reported by Landovitz et al.[15] The study protocol was approved by the institutional review board or ethics committee at each participating site, and all participants provided written informed consent. Plasma samples were obtained from HIV-uninfected men and women who enrolled in the HPTN 077 study. All participants were given the option to participate in the pharmacogenomic study by providing specific informed consent. For the samples analyzed in the present study, active arm participants (n = 68) in both cohorts, cohorts 1 and 2, received oral tablets (30 mg) for 4 weeks, followed by a 1-week wash out period. Participants in cohort 1 (n = 37) received 3 intramuscular injections containing CAB every 12 weeks whereas cohort 2 participants (n = 31) were given 5 CAB-containing intramuscular injections at 4-week intervals between the first and second injections and 8-week intervals between the remaining injections. Following the oral lead-in phase, plasma samples used for metabolite analysis were collected at 1 week after the last oral dose. Participants in cohort 1 received two intramuscular injections of long-acting CAB (800 mg of CAB administered as two 400 mg injections) whereas study participants in cohort 2 were given a single intramuscular injection of long-acting CAB (600 mg) at each administration. For CAB-glucuronide analysis, postinjection plasma samples were collected at 1 week and 4 weeks after the first injection in both cohorts.

Measurement of CAB-Glucuronide Plasma Concentrations. Liquid chromatography coupled to tandem mass spectrometry (LC−MS/MS) was employed to measure plasma concentrations of CAB-glucuronide. Thawed plasma (100 μL) was extracted using acetonitrile to precipitate proteins. Next, samples were placed on ice for 10 min and centrifuged at 12 000 × g at 4 °C for 10 min. The supernatants were collected, dried under vacuum, and reconstituted in 40 μL of methanol. Aliquots (10 μL) of the reconstituted samples were analyzed using a Dionex Ultimate 3000 UHPLC system equipped with a Waters Acquity UPLC BEH C_{18} column (1.7 μm particles, 3.0 mm × 150 mm). The binary mobile phase of 0.4% formic acid in water (A) and 25 mM ammonium formate in acetonitrile−water (80:20, v/v) (B) was used as previously

https://dx.doi.org/10.1021/acsptsci.0c00181
ACS Pharmacol. Transl. Sci. 2021, 4, 226−239

reported.[10] The gradient program was as follows: flow rate of 0.55 mL/min; linear gradient, 0−0.2 min, 45% B; 0.2−5.0 min, 45−62% B; 5.0−6.1 min, 62−90% B; 6.1−7.1 min, 90% B; 7.1−8 min, 90−45% B. The analytes were detected by using a TSQ Vantage Triple-Stage Quadrupole mass spectrometer (Thermo Scientific, Pittsburgh, PA) operated in positive ion mode equipped with an electrospray source via selected reaction monitoring (SRM, CAB-glucuronide ion transition m/z 582.0 → 406.0). A calibration curve for CAB-glucuronide was generated using a synthetic standard of CAB-glucuronide (calibration standards were prepared in blank human plasma at a total volume of 100 μL) at 9 concentrations ranging from 25 000 ng/mL to 0.25 ng/mL. CAB-glucuronide levels in the samples were calculated by interpolating the generated calibration curve using GraphPad Prism (San Diego, CA). The same LC conditions were employed for the analysis of DTG-glucuronide and RAL-glucuronide in cell-based assays. For the analysis of RXF-glucuronide and SN-38-glucuronide, the following gradient was used: flow rate of 0.6 mL/min; linear gradient, 0−12 min, 25−70% B; 12−12.1 min, 70−90% B; 12.1−13 min, 90% B; and 13−14 min, 90−25% B. The SRM ion transitions used for the detection of the glucuronide conjugates of DTG, RAL, RXF, and SN-38 were m/z 596.1 → 420.1, 621.1 → 445.1, 650.2 → 474.2, and 569.1 → 393.1, respectively.

The limits of detection (LOD) and quantification (LOQ) were calculated using the relationship between the residual standard deviation (SD) of the calibration curve and its slope (S), as suggested by the ICH standard (International Conference on Harmonization of Technical Requirements for Registration of Pharmaceuticals for Human Use). The values for LOD and LOQ were calculated using the following equations: LOD = (3.3 × SD/S) and LOQ = (10 × SD/S). The limit of quantitation for CAB-glucuronide in plasma samples was 2.17 ng/mL.

Statistical Analysis. Statistical analyses were performed using GraphPad Prism (San Diego, CA). Differences in CAB-glucuronide levels between the wild-type and predicted deleterious variants were analyzed using a two-tailed unpaired t test. The significance was denoted as follows: *, $p \leq 0.05$; **, $p \leq 0.01$; ***, $p \leq 0.001$.

Human Liver and Kidney Microsome Metabolism Experiments. Human liver microsomes (pooled from 50 mixed sex donors) were purchased from Sekisui XenoTech, LLC, (Kansas City, KS) whereas human kidney microsomes (pooled from 5 mixed sex donors) were obtained from BIOIVT (Baltimore, MD). Microsomes (0.5 mg/mL) were preincubated with CAB (10 μM) at 37 °C in a water bath for 5 min in 100 mM potassium phosphate buffer, pH 7.4, prior to the addition of a UGT reaction mixture (Corning Gentest, Discovery Labware, Woburn, MA) containing 25 mM uridine 5′-diphosphoglucuronic acid (UDPGA) and alamethicin. The reaction volume was 250 μL, and reactions were allowed to proceed for 60 min at 37 °C. At the end of the incubations, the reactions were quenched with 250 μL of acetonitrile followed by centrifugation at 10 000g at 4 °C for 10 min. Next, the supernatants were dried under vacuum and subsequently reconstituted in 50 μL of methanol. Samples were analyzed using LC−MS/MS as described above.

Genomic DNA isolation. Genomic DNA was isolated from 5.0 mL of cell-free plasma using a *Quick*-cfDNA Serum & Plasma kit (Zymo Research Corp., Irvine, CA). Purified DNA was eluted using 40 μL of elution buffer.

Sample Preparation for Next-Generation Sequencing. Samples were prepared following the Illumina low input library preparation guide (Illumina, San Diego, CA). The libraries were pooled, and a cleanup procedure was performed using the Illumina sample purification beads. The final pooled DNA library (5 μL) was diluted in 985 μL of HT1 hybridization buffer and spiked with 20% PhiX. Sequencing was performed using an amplicon size of 150 base pair reads. At least one technical control was included per sample batch.

Next-Generation Sequencing Targeted Enrichment Design and Data Analysis. Sequencing was performed using the Illumina TruSeq custom amplicon v2.0 kit (San Diego, CA). Custom probes targeting the exonic regions of *UGT1A1* and *UGT1A9* were designed *in silico* using the Illumina DesignStudio software. Specific chromosomal design coordinates can be accessed using the DesignStudio ID 108784. Target enrichment design and data analysis were performed as previously described.[22] The phenotypic consequence of missense variants was assigned using SIFT (Sorts Intolerant From Tolerant substitutions; J. Craig Venter Institute online tool) and PolyPhen (Polymorphism phenotyping; Harvard University online tool) *in silico* prediction tools where amino acid substitutions were scored.

Site-Directed Mutagenesis and Expression of UGT1A1 and UGT1A1 P152T. The full-length cDNA of human UGT1A1 was purchased from OriGene (Rockville, MD). The following primers were used to generate a *UGT1A1 454C>A* construct for UGT1A1 P152T expression: 5′-CTGCAAGGAAGGAAAGTGTCCGTCAGCATGACA-3′ and 5′-TGTCATGCTGACGGACACTTTCCTTCCTTG-CAG-3′. A QuickChange lightning site-directed mutagenesis kit (Agilent Technologies, Cedar Creek, TX) was used following the manufacturer's protocol. A GeneJET Plasmid Miniprep Kit (Thermo Fisher Scientific, Waltham, MA) was used to isolate plasmid DNA, and the presence of the desired UGT1A1 mutation was confirmed by DNA sequencing. The DNA (4 μg) was transfected into COS-7 cells using Lipofectamine 3000 (Invitrogen, Carlsbad, CA) following the manufacturer's instructions.

Glucuronidation by UGT1A1 and UGT1A1 P152T Expressed in COS-7 Cells. At a time 48 h after transfection, COS-7 cells were treated with each drug separately (CAB/DTG/RAL/RXF/SN-38) at a final concentration of 20 μM in 1 mL of Dulbecco's modified Eagle's medium (Gibco, Thermo Fisher Scientific) per well. Drug treated COS-7 cells were incubated at 37 °C in an atmosphere of >95% humidity and 5% carbon dioxide for 24 h. After the incubation, 500 μL of media were mixed with 500 μL of acetonitrile followed by vortexing and centrifugation at 10 000g at 4 °C for 10 min. The resulting supernatants were collected, dried under vacuum (using a Vacufuge plus, Eppendorf), and reconstituted in 100 μL of methanol. LC−MS/MS analyses were performed as described above. The IC_{50} values of DTG, RAL, RXF, and SN-38 were determined using the CellTiter-Glo luminescent cell viability assay kit (Promega Corporation, Madison, WI) according to the manufacturer's instructions.

Site-Directed Mutagenesis and Expression of UGT1A9, UGT1A9 H217Y, and UGT1A9 R464G. The full-length cDNA of human UGT1A9 was obtained from OriGene (Rockville, MD). Constructs for use in expressing UGT1A9 H217Y and UGT1A9 R464G were generated using the following primers: for UGT1A9 H217Y expression, 5′-AAAAACGGTGGCATAATAAATATTCCTCCAAGTG-

https://dx.doi.org/10.1021/acsptsci.0c00181
ACS Pharmacol. Transl. Sci. 2021, 4, 226−239

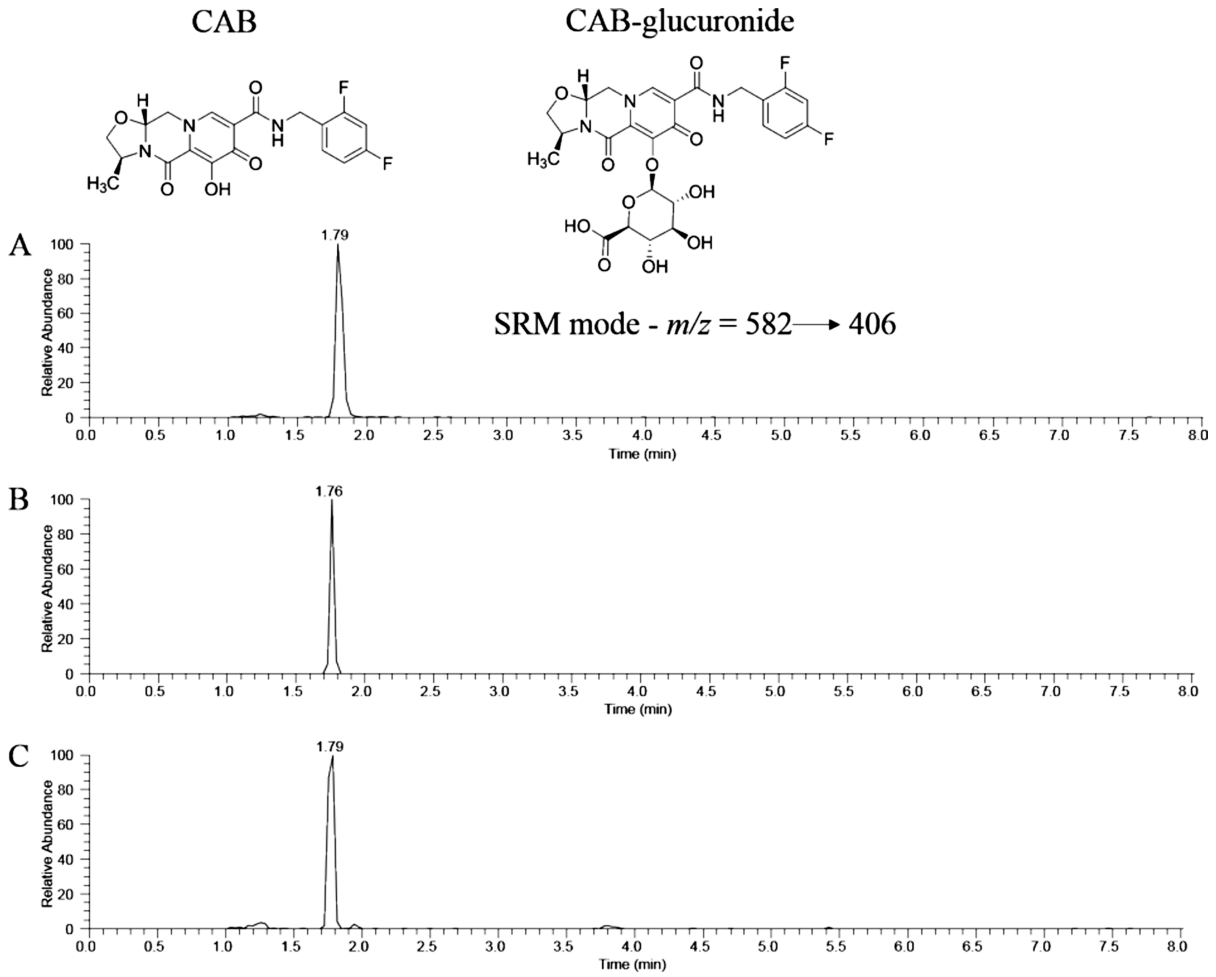

Figure 1. Chemical structures of CAB, CAB-glucuronide, and extracted ion chromatograms of CAB-glucuronide. CAB-glucuronide ion chromatogram in selected reaction monitoring (SRM) mode for the ion transition m/z 582 → 406 in (A) synthetic standard, (B) *in vitro* liver microsome assay, and (C) plasma sample of an HPTN 077 participant following CAB administration. For *in vitro* assays, CAB and human liver microsomes were incubated at 37 °C for 60 min in the presence of a UGT reaction mixture containing UDPGA.

CATGATGTG-3′ and 5′- CACATCATGCACTTGGAG-GAATATTTATTATGCCACCGTTTTT-3′. For UGT1A9 R464G expression, 5′- CGCGCCCTTGTGCCCCATCA-CAAACTCCA-3′ and 5′-TGGAGTTTGTGATGGGGCA-CAAGGGCGCG-3′. Site-directed mutagenesis was carried out as described above. For COS-7 cell-based CAB glucuronidation assays, drug treatments were performed using two time points: 24 and 48 h.

Immunoblot Analysis. COS-7 cells were harvested in 500 μL of phosphate-buffered saline (Gibco, Thermo Fisher Scientific) followed by centrifugation at 3000*g* for 5 min at 4 °C. Cell lysis buffer containing freshly added phosphatase and protease inhibitor cocktail (Thermo Fisher Scientific) and phenylmethylsulfonyl fluoride was used to resuspend the cell pellets. This was followed by passage of the resuspended cell pellets (35 times) through a syringe (needle gauge 27G) for lysis and centrifugation at 14 000*g* for 10 min at 4 °C. Protein concentrations were determined using a bicinchoninic acid assay kit according to manufacturer's instructions (Thermo Fisher Scientific). A total of 25 μg of proteins was loaded onto a 4−15% sodium dodecyl sulfate-polyacrylamide gel (Biorad, Hercules, CA), blotted onto a nitrocellulose membrane (Invitrogen, Carlsbad, CA), and then incubated with a human anti-UGT1A1 antibody (Abcam, Cambridge, MA), anti-MYC (myelocytomatosis C-terminal) antibody (Millipore Sigma, St. Louis, MO), or a human anti-UGT1A9 antibody (Abcam, Cambridge, MA). Similarly, a human anti-GAPDH antibody was used to detect GAPDH as a loading control. A ChemiDoc Touch imaging system (Biorad, Hercules, CA) was used for chemiluminescent imaging of the blots.

RESULTS

In Vitro CAB Metabolism. To establish our detection method prior to the analysis of plasma samples of HPTN 077 participants, CAB metabolism assays were performed using human liver microsomes. We initially utilized an untargeted LC−MS/MS approach to detect metabolites. Through these studies, a metabolite at m/z 582 was detected, and it was only present in the reactions containing the UGT cofactor, uridine 5′-diphospho-glucuronic acid. Based on retention time and fragmentation pattern, this metabolite was identified as CAB-glucuronide (Figure 1). The MS/MS fragmentation spectrum of this compound exhibited a major mass fragment ion at m/z 406 suggesting the loss of the glucuronide group. Therefore, for subsequent experiments, the levels of the CAB-glucuronide metabolite were monitored via selected reaction monitoring using the ion transition, parent mass → product ion: m/z 582 → 406. Of note, no additional metabolites of CAB were

https://dx.doi.org/10.1021/acsptsci.0c00181
ACS Pharmacol. Transl. Sci. 2021, 4, 226−239

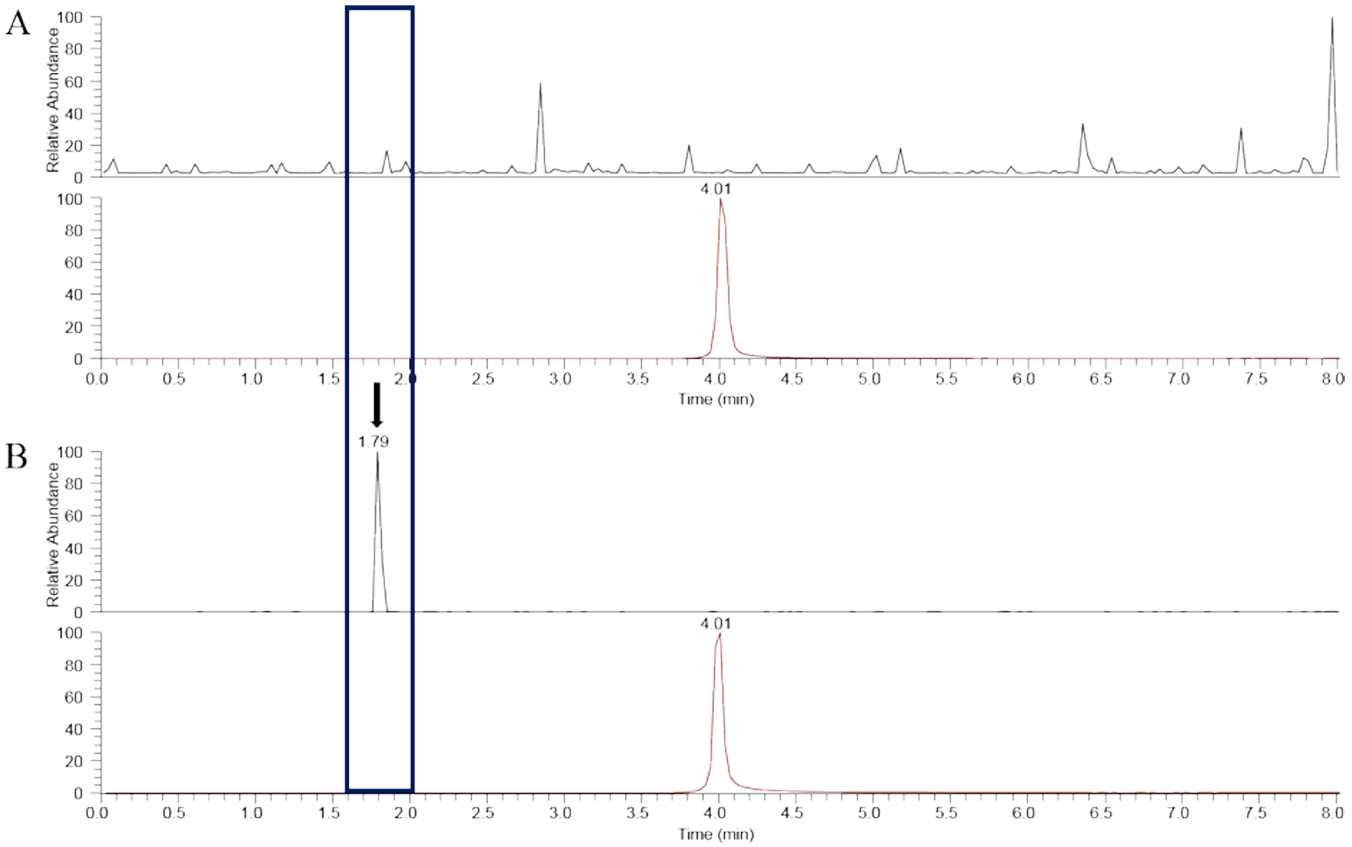

Figure 2. CAB-glucuronide is formed using human kidney microsomes. Extracted ion chromatograms of CAB-glucuronide (upper panel; retention time 1.79 min) and CAB (lower panel; 4.01 min) in the (A) absence (control experiment) and (B) presence of the UDPGA. An arrow indicates the peak corresponding to CAB-glucuronide. CAB and human kidney microsomes were incubated at 37 °C in the absence or presence of UDPGA for 60 min.

detected in these studies. Further, since kidneys may contribute to metabolism following intramuscular injection, we tested whether CAB could be metabolized in the kidney. To do so, we employed human kidney microsomes. From these experiments, we observed the formation of CAB-glucuronide in the incubations that contained human kidney microsomes and UGT cofactor (Figure 2). We did not detect any other CAB metabolites from these *in vitro* incubations.

Analysis of Genetic Variants in the Genes Encoding *UGT1A1* and *UGT1A9*. In order to investigate the variants within the genes encoding enzymes that are responsible for CAB metabolism, we performed targeted sequencing of *UGT1A1* and *UGT1A9*. The demographic details of participants in this study are listed in Table 1. A total of 36 single nucleotide variants and deletions that cause an amino acid substitution in the UGT1A1 protein were detected in 33 participants (Table 2). Of these 36 variants, 24 have not been previously reported. Using *in silico* tools, SIFT and PolyPhen, 10 of the detected missense variants were predicted to have a deleterious and damaging impact on UGT1A1 protein function (Table 2). Of the 68 participants genotyped, 13 carried variants in *UGT1A1* that were predicted to have a deleterious and damaging impact on the UGT1A1 protein (13/68 individuals; 19.1%). Further, 5 of 68 (7.3%) participants carried an unreported variant translating to a proline to threonine substitution at amino acid 152 of the UGT1A1 protein (UGT1A1 P152T) that was predicted to be deleterious. Another unreported *UGT1A1* missense variant was detected in 7 individuals (10.3%) and was predicted to result in substitution of amino acid 478 of the UGT1A1 protein, substituting a valine residue for an alanine residue (UGT1A1 A478 V). This variant was predicted to be tolerated. We detected 12 previously reported *UGT1A1* variants: 1349G > A, 1348C > T, 1325G > A, 253A > G, 673G > A, 233C > T, 686C > A, 1373C > T, 1492G > A, 577G > A, 1429G > A, and 120G > A. Of these, the *UGT1A1* variant rs200370335 (NM_000463.2:c.1349G>A) was detected in 3 individuals and is predicted to be deleterious, yielding a 4.4% (3/68) observed frequency of this variant. Another *UGT1A1* variant rs35350960 (NM_000463.2:c.686C>A) was detected at an observed frequency of 2.9% (2/68 individuals) and is predicted to be tolerated. All individuals carrying *UGT1A1* variants were heterozygous.

For *UGT1A9*, a total of 37 single nucleotide variants and deletions that cause a substitution at the amino acid level in the UGT1A9 protein were detected in 37 participants: 30 enrolled in the USA study sites and 7 in South Africa (Table 3). Using *in silico* tools, SIFT and PolyPhen, 12 participants were predicted to carry missense variants with a deleterious and damaging impact on UGT1A9 protein function (Table 3). One previously unreported variant was detected in 14 individuals and predicted to affect amino acid 217 of the UGT1A9 protein resulting in a substitution of the histidine residue to a tyrosine residue (UGT1A9 H217Y, 20.6% observed frequency, 14/68 individuals). This *UGT1A9* variant was predicted to be tolerated. Additionally, another unreported variant translating to an alanine to valine substitution at amino acid 475 of the UGT1A9 protein was predicted to be tolerated,

https://dx.doi.org/10.1021/acsptsci.0c00181
ACS Pharmacol. Transl. Sci. 2021, 4, 226−239

Table 1. Baseline Demographic Details of the Participants in Cohort 1 and Cohort 2

	overall	cohort 1	cohort 2
Age			
18–25	21/68 (30.9%)	8/37 (21.6%)	13/31 (41.9%)
26–35	27/68 (39.7%)	15/37 (40.5%)	12/31 (38.7%)
36–45	7/68 (10.3%)	4/37 (10.8%)	3/31 (9.7%)
46–55	8/68 (11.8%)	6/37 (16.2%)	2/31 (6.5%)
56–65	5/68 (7.4%)	4/37 (10.8%)	1/31 (3.2%)
mean (SD)	33 (12.0)	36 (12.8)	30 (10.5)
median	29	32	29
25th, 75th percentile	24, 39	26, 48	23, 33
min, max	18, 62	19, 60	18, 62
Sex at Birth			
male	28/68 (41.2%)	15/37 (40.5%)	13/31 (41.9%)
female	40/68 (58.8%)	22/37 (59.5%)	18/31 (58.1%)
Weight (kg)			
N	68	37	31
mean (SD)	81 (20.7)	82 (19.4)	80 (22.5)
median	79	79	78
25th, 75th percentile	67, 97	70, 97	61, 97
min, max	43, 127	43, 122	47, 127
BMI			
N	68	37	31
mean (SD)	28 (7.0)	29 (6.9)	28 (7.1)
median	26	26	26
25th, 75th percentile	22, 34	24, 33	21, 35
min, max	16, 50	16, 50	17, 44

	overall	cohort 1	cohort 2
Race			
Latino	11/68 (16.2%)	7/37 (18.9%)	4/31 (12.9%)
nonhispanic Asian	1/68 (1.5%)	0/37 (0.0%)	1/31 (3.2%)
nonhispanic black	23/68 (33.8%)	9/37 (24.3%)	14/31 (45.2%)
nonhispanic white	30/68 (44.1%)	21/37 (56.8%)	9/31 (29.0%)
nonhispanic mixed/other	3/68 (4.4%)	0/37 (0.0%)	3/31 (9.7%)
Smoking			
no	58/68 (85.3%)	31/37 (83.8%)	27/31 (87.1%)
yes	10/68 (14.7%)	6/37 (16.2%)	4/31 (12.9%)
Region			
U.S.	53/68 (77.9%)	32/37 (86.5%)	21/31 (67.7%)
South Africa	15/68 (22.1%)	5/37 (13.5%)	10/31 (32.3%)
Brazil	0/68 (0.0%)	0/37 (0.0%)	0/31 (0.0%)

with 8 participants carrying this mutant (UGT1A9 A475 V, 11.8% frequency, 8/68 individuals). Thirteen previously reported *UGT1A9* variants were detected: 1340G > A, 1339C > T, 1316G > A, 850C > T, 764C > T, 281C > T, 665G > A, 1364C > T, 8G > A, 454A > G, 215G > A, 1483G > A, and 1420G > A. Of these, two previously reported *UGT1A9* variants, rs750374477 (NM_021027.3:c.850C>T) and rs145084767 (NM_021027.3:c.8G>A) were each found at an observed frequency of 2.9% (2/68 individuals). Both variants are predicted to be tolerated. All participants carrying *UGT1A9* variants were heterozygous.

Correlation between CAB-Glucuronide Plasma Levels and *UGT1A1/UGT1A9* Genotype. We investigated potential correlations between CAB-glucuronide levels and the *UGT1A1/UGT1A9* genotype. Of the 68 participants, 35 (51.5%, 35/68 individuals) were wild-type for *UGT1A1* while 33 (48.5%, 33/68 individuals) participants carried *UGT1A1* variants. Of the 35 wild-type participants, 21 participants (60%, 21/35 individuals) had detectable levels of CAB-glucuronide in their plasma samples 1 week after the oral lead-in phase. Nineteen participants (54.3%, 19/35 individuals) showed quantifiable CAB-glucuronide levels with a mean value of 22.63 ± 57.41 ng/mL (Figure 3A). At 1-week postinjection, CAB-glucuronide was detectable in all participants (100%, 35/35 individuals) that were homozygous wild-type for *UGT1A1* with a mean value of 63.14 ± 76.16 ng/mL (Figure 3A). Similarly, all these above-mentioned *UGT1A1* homozygous wild-type participants (100%, 35/35 individuals) had detectable CAB-glucuronide levels at 4 weeks after the first injection, and the mean value was 37.95 ± 25.44 ng/mL (Figure 3A).

Of the 33 participants carrying *UGT1A1* variants, 13 (39.4%, 13/33) individuals carried *UGT1A1* variants that were predicted to be deleterious. Interestingly, only 5 (38.5%, 5/13 individuals) of these participants who carried predicted deleterious *UGT1A1* variants had detectable CAB-glucuronide levels 1 week after the oral phase. We were able to quantify CAB-glucuronide levels in these participants, and the mean value was 6.63 ± 4.49 ng/mL (Figure 3A). In contrast, CAB-glucuronide was detected in all 13 (100%, 13/13) participants who carried predicted deleterious *UGT1A1* variants with a mean value of 40.16 ± 43.05 ng/mL at 1-week postinjection (Figure 3A). At 4 weeks after the first injection, all 13 participants had CAB-glucuronide in plasma, and the mean value was 27.38 ± 26.32 ng/mL (Figure 3A).

A total of 31 (45.6%, 31/68) participants were homozygous wild-type for *UGT1A9*, while 37 (54.4%, 37/68) participants were heterozygous for *UGT1A9* variants. Of the 31 wild-type participants, 16 (51.6%, 16/31) had detectable CAB-glucuronide levels 1 week after the oral phase with a mean value of 28.13 ± 66.60 ng/mL (Figure 3B). At 1-week postinjection, all 31 (100%, 31/31) participants showed detectable CAB-glucuronide levels, and the mean value was 55.09 ± 76.62 ng/mL (Figure 3B). CAB-glucuronide was detected in all 31 participants at 4 weeks after the first injection with a mean plasma level of 36.39 ± 27.25 ng/mL (Figure 3B).

Of the 37 individuals carrying *UGT1A9* variants, 12 carried *UGT1A9* variants that were predicted to be deleterious. Six (50%, 6/12) participants who carried *UGT1A9* variants that were predicted to be deleterious had detectable levels of CAB-glucuronide in their plasma samples 1 week after the oral phase. The mean CAB-glucuronide level was 5.42 ± 1.74 ng/mL (Figure 3B). At 1-week postinjection, we detected CAB-glucuronide in all 12 of these participants for a mean concentration of 54.20 ± 43.23 ng/mL (Figure 3B). All 12 participants exhibited detectable levels of CAB-glucuronide at 4 weeks after the first injection, and the mean concentration was 35.51 ± 26.37 ng/mL (Figure 3B).

Impact of the UGT1A1 P152T Mutant on Drug Glucuronidation. Five individuals carried a previously unreported variant that was predicted to be deleterious, *UGT1A1 454C>A*. This mutation results in an amino acid

https://dx.doi.org/10.1021/acsptsci.0c00181
ACS Pharmacol. Transl. Sci. 2021, 4, 226–239

Table 2. *UGT1A1* Missense Variants Detected in HPTN-077 Participants[a]

geographic location	variant (ref > alt)	cDNA position	coding DNA sequence position	protein position	amino acid substitution (ref > alt)	SIFT prediction	PolyPhen prediction
Chapel Hill	G > A	296	281	94	S > N	tolerated (0.41)	benign (0.008)
Chapel Hill	A > G	1414	1399	467	R > G	deleterious (0)	probably damaging (0.994)
Chapel Hill	G > A	1364	1349	450	R > H	deleterious (0)	probably damaging (1)
Chapel Hill	C > T	1363	1348	450	R > C	deleterious (0)	probably damaging (1)
Chapel Hill	G > A	1340	1325	442	R > H	tolerated (0.6)	benign (0.415)
Chapel Hill	T > C	74	59	20	L > P	deleterious (0.01)	possibly damaging (0.1)
Chapel Hill	A > G	268	253	85	R > G	tolerated (0.07)	benign (0.003)
Chapel Hill	C > T	1517	1502	501	T > I	tolerated (0.98)	benign (0.128)
Los Angeles	G > A	340	325	109	V > M	tolerated (0.24)	benign (0.063)
Los Angeles	C > T	1448	1433	478	A > V	tolerated (0.06)	probably damaging (1)
Los Angeles	T > C	59	44	15	L > P	deleterious (0)	possibly damaging (0.902)
Los Angeles	C > A	469	454	152	P > T	deleterious (0.02)	probably damaging (0.998)
Los Angeles	G > A	688	673	225	V > M	tolerated (0.17)	benign (0.025)
Los Angeles	C > T	248	233	78	T > M	tolerated (0.08)	benign (0.223)
San Francisco	C > T	536	521	174	A > V	deleterious (0.02)	benign (0.005)
San Francisco	C > A	377	362	121	A > D	tolerated (0.68)	benign (0.012)
San Francisco	G > A	1544	1529	510	C > Y	deleterious (0.01)	possibly damaging (0.624)
San Francisco	C > A	701	686	229	P > Q	tolerated (0.23)	possibly damaging (0.862)
San Francisco	G > A	520	505	169	V > I	tolerated (0.13)	possibly damaging (0.776)
San Francisco	C > T	1388	1373	458	A > V	deleterious (0)	probably damaging (1)
San Francisco	C > T	1468	1453	485	Q > *	N/A	N/A
Washington, DC	C > A	478	463	155	P > T	deleterious (0.03)	benign (0.168)
Washington, DC	C > T	409	394	132	H > Y	tolerated (1)	benign (0.006)
Washington, DC	G > A	19	4	2	A > T	tolerated - low confidence (0.16)	possibly damaging (0.811)
Johannesburg	G > A	202	187	63	D > N	deleterious (0.01)	benign (0.014)
Johannesburg	G > A	1507	1492	498	V > I	tolerated (1)	benign (0.007)
Johannesburg	A > G	247	232	78	T > A	tolerated (0.06)	benign (0.033)
Johannesburg	G > A	592	577	193	V > M	deleterious (0.01)	probably damaging (0.984)
Johannesburg	G > A	125	110	37	G > D	deleterious (0)	probably damaging (0.998)
Johannesburg	G > A	1444	1429	477	A > T	deleterious (0.01)	probably damaging (1)
Johannesburg	A > T	416	401	134	K > M	deleterious (0.01)	possibly damaging (0.806)
Johannesburg	T > G	1525	1510	504	F > V	deleterious (0.03)	probably damaging (0.989)
Johannesburg	T > C	155	140	47	I > T	deleterious (0.03)	benign (0.014)
Johannesburg	G > A	135	120	40	W > *	N/A	N/A
Durban	G > A	1504	1489	497	A > T	tolerated (0.2)	possibly damaging (0.718)
Durban	C > T	1427	1412	471	A > V	deleterious (0)	probably damaging (1)

[a]Two *in silico* tools: SIFT and PolyPhen were used to predict the functional consequence of resulting amino acid mutations. A SIFT score <0.05 was indicative of a damaging amino acid substitution and >0.05 a tolerated substitution. A PolyPhen score >0.908 was suggestive of a probably damaging, 0.447-0.908 a possible damaging, or <0.447 a benign amino acid substitution. Deleterious and probably damaging *UGT1A1* missense variants was observed at a frequency of 19.1% (13/68 individuals).

substitution from proline to threonine at residue 152 of the UGT1A1 protein. In order to functionally test the impact of the UGT1A1 P152T mutant on drug glucuronidation, we generated a *UGT1A1 454C>A* construct and transfected it into COS-7 cells. Similarly, wild-type UGT1A1 was transfected separately into COS-7 cells to allow for comparisons of the

https://dx.doi.org/10.1021/acsptsci.0c00181
ACS Pharmacol. Transl. Sci. 2021, 4, 226−239

Table 3. *UGT1A9* Missense Variants Detected in HPTN-077 Participants[a]

geographic location	variant (ref > alt)	cDNA Position	coding DNA sequence position	protein position	amino acid substitution (ref > alt)	SIFT prediction	PolyPhen prediction
Chapel Hill	G > A	1377	1340	447	R > H	deleterious (0)	probably damaging (0.999)
Chapel Hill	C > T	1376	1339	447	R > C	deleterious (0)	probably damaging (0.999)
Chapel Hill	G > A	1353	1316	439	R > H	tolerated (0.07)	benign (0.056)
Chapel Hill	A > G	1427	1390	464	R > G	deleterious (0)	probably damaging (0.999)
Chapel Hill	C > T	881	844	282	P > S	deleterious (0)	benign (0.02)
Chapel Hill	T > C	525	488	163	L > P	deleterious (0)	probably damaging (0.991)
Chapel Hill	G > A	467	430	144	A > T	deleterious (0.01)	probably damaging (0.954)
Chapel Hill	C > T	1530	1493	498	T > I	tolerated (1)	benign (0.272)
Los Angeles	C > T	887	850	284	P > S	tolerated (1)	benign (0.011)
Los Angeles	C > T	1461	1424	475	A > V	tolerated (0.08)	probably damaging (0.999)
Los Angeles	C > T	194	157	53	H > Y	deleterious (0)	probably damaging (0.995)
Los Angeles	C > T	468	431	144	A > V	tolerated (1)	probably damaging (0.967)
San Francisco	C > T	801	764	255	T > M	tolerated (0.15)	benign (0.054)
San Francisco	C > T	1401	1364	455	A > V	deleterious (0)	probably damaging (0.999)
San Francisco	G > A	702	665	222	R > H	tolerated (0.22)	benign (0.001)
San Francisco	C > T	318	281	94	A > V	tolerated (0.32)	benign (0.007)
San Francisco	C > T	686	649	217	H > Y	tolerated (1)	benign (0.005)
San Francisco	G > T	50	13	5	G > W	deleterious (0.03)	possibly damaging (0.576)
San Francisco	G > A	774	737	246	S > N	tolerated (1)	benign (0.107)
San Francisco	C > T	185	148	50	L > F	deleterious (0.01)	benign (0.435)
San Francisco	G > A	578	541	181	A > T	tolerated (1)	benign (0.07)
San Francisco	C > T	674	637	213	H > Y	tolerated (1)	benign (0.009)
San Francisco	A > G	873	836	279	Q > R	tolerated (0.36)	benign (0.008)
San Francisco	G > A	240	203	68	R > K	tolerated (0.34)	benign (0.002)
San Francisco	G > A	1557	1520	507	C > Y	deleterious (0.01)	probably damaging (0.999)
San Francisco	W > *	55	18	6	W > *	N/A	N/A
San Francisco	Q > *	1481	1444	482	Q > *	N/A	N/A
Washington, DC	G > A	45	8	3	C > Y	tolerated (0.07)	benign (0.002)
Washington, DC	A > G	491	454	152	N > D	deleterious (0)	benign (0.002)
Washington, DC	G > A	252	215	72	C > Y	tolerated (1)	benign (0.012)
Johannesburg	G > A	1520	1483	495	V > I	tolerated (1)	benign (0.004)
Johannesburg	G > A	1457	1420	474	A > T	deleterious (0.01)	probably damaging (0.999)
Johannesburg	T > G	1538	1501	501	F > V	deleterious (0.03)	probably damaging (0.999)
Johannesburg	G > A	104	67	23	A > T	tolerated (1)	benign (0.056)
Johannesburg	G > T	576	539	180	G > V	deleterious (0.04)	probably damaging (0.955)
Durban	G > A	1517	1480	494	A > T	tolerated (0.16)	probably damaging (0.956)
Durban	C > T	1440	1403	468	A > V	deleterious (0)	probably damaging (0.999)

[a]Two *in silico* tools: SIFT and PolyPhen were used to predict the functional consequence of resulting amino acid mutations. A SIFT score <0.05 was indicative of a damaging amino acid substitution and >0.05 a tolerated substitution. A PolyPhen score >0.908 was suggestive of a probably damaging, 0.447−0.908 a possible damaging, or <0.447 a benign amino acid substitution. Deleterious and probably damaging *UGT1A9* missense variants were observed at a frequency of 17.6% (12/68 individuals).

https://dx.doi.org/10.1021/acsptsci.0c00181
ACS Pharmacol. Transl. Sci. 2021, 4, 226−239

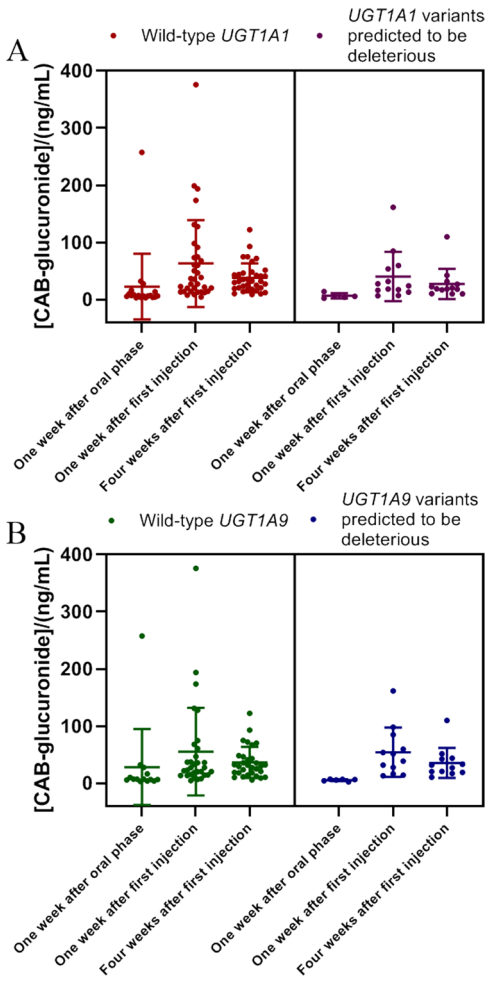

Figure 3. Relationship between CAB-glucuronide plasma levels and *UGT1A1* or *UGT1A9* genotype of HPTN 077 participants. (A) Participants were grouped by *UGT1A1* genotype: wild type (n = 35) versus predicted deleterious variants (n = 13). (B) Participants were grouped by *UGT1A9* genotype: wild type (n = 31) versus predicted deleterious variants (n = 12). CAB-glucuronide concentrations in plasma samples following the oral dosing period (samples collected 1 week after the oral lead-in phase) and injection phase (samples collected at 1 week and 4 weeks after the first injection) were then plotted against genotype for each participant. The observed differences were not statistically significant.

activities of wild-type UGT1A1 versus UGT1A1 P152T. Immunoblotting confirmed the expression of both wild-type UGT1A1 and UGT1A1 P152T in the transfected cells (Figure 4). Next, the abilities of wild-type UGT1A1 and UGT1A1 P152T to glucuronidate CAB, DTG, RAL, RXF, and SN-38 were measured. Following 24 h of treatment, glucuronidated metabolites of CAB, DTG, and RAL were undetectable in cells expressing UGT1A1 P152T, whereas these drugs were readily glucuronidated in cells transfected with wild-type UGT1A1 (Figure 4). Additionally, a marked reduction in the glucuronidation of both RXF and SN-38 was observed in cells transfected with UGT1A1 P152T as compared to those transfected with wild-type UGT1A1 (Figure 4). Assays were also performed to test the impact of the above-mentioned drugs on COS-7 cell viability. In these studies, the IC_{50} values for RXF, DTG, RAL, and SN-38 were 20.1 μM, 360.4 μM, 36.4 μM, and 131.4 μM, respectively.

Activity of UGT1A9 H217Y and UGT1A9 R464G toward CAB. The potential impact of two UGT1A9 mutants, UGT1A9 H217Y (a mutant predicted to be tolerated) and UGT1A9 R464G (a mutant predicted to be deleterious) on CAB glucuronidation was investigated using COS-7 cells expressing UGT1A9 wild-type, UGT1A9 H217Y, or UGT1A9 R464G. Following 24 h of incubation with CAB, formation of CAB-glucuronide was not observed in the UGT1A9 wild-type, UGT1A9 H217Y, or UGT1A9 R464G assays (data not shown). However, after 48 h treatments with CAB, we were able to detect CAB-glucuronide production by the cells expressing UGT1A9 wild-type and UGT1A9 H217Y. In contrast, in the UGT1A9 R464G incubations, production of CAB-glucuronide was not detectable above the background (Figure 5).

DISCUSSION

Based on previous *in vitro* reaction phenotyping studies using human liver microsomes and recombinant UGT enzymes, it has been reported that UGT1A1 and UGT1A9 are the primary enzymes that metabolize CAB.[10] Glucuronidation is mainly associated with the clearance of orally administrated drugs, and the role of this pathway in the metabolism of drugs delivered via other routes such as intramuscular injections is largely unexplored. In our study, CAB-glucuronide was detected in plasma samples of all the participants following intramuscular injection of long-acting CAB. This agrees with previously published findings demonstrating the detection of CAB-glucuronide following subcutaneous or intramuscular injections.[10] According to previous studies, long-acting CAB has an elimination half-life of 25−54 days.[23,24] Extrahepatic organs such as kidney may contribute to CAB glucuronidation in this context. Data from our *in vitro* assays using human kidney microsomes indicate that CAB could be metabolized in the kidney. This observation is concordant with recently reported work by Liu et al.[19] Additionally, it is well established that the UGT enzymes responsible for CAB metabolism, UGT1A1 and UGT1A9, are expressed differentially in the liver and kidney.[20,25,26] Specifically, UGT1A1 is more abundant in the liver whereas UGT1A9 is highly expressed in the kidney (approximately 4-fold higher than in the liver).[25] The relative contributions of each of these UGTs may differ following oral administration versus intramuscular injection.

Through this work, we identified 36 *UGT1A1* variants, 67% of which were previously unreported. Additionally, we detected 37 *UGT1A9* variants, 65% of which were novel. A total of 13 participants carried *UGT1A1* variants predicted to have a deleterious and damaging impact on UGT1A1 activity. Of these, 5 participants from three study sites, Los Angeles, Washington, DC and Johannesburg carried a previously unreported *UGT1A1 454C>A* variant that was predicted to be deleterious. Translation of this *UGT1A1* gene variant results in an amino acid substitution at residue 152 of the UGT1A1 protein, predicted to be located six amino acid residues away from a buried α-helix.[27] The substitution of proline to threonine at this position, P152T, changes the residue from the nonpolar, aliphatic side chain (proline) to a polar, uncharged side chain containing a hydroxyl group (threonine). In order to test activity of UGT1A1 P152T, we introduced the mutation into a *UGT1A1* construct and transfected it into COS-7 cells. COS-7 cell-based assays have been previously used to investigate activities of UGTs.[28,29] Based on our data, we observed that UGT1A1 P152T did not exhibit activity

https://dx.doi.org/10.1021/acsptsci.0c00181
ACS Pharmacol. Transl. Sci. 2021, 4, 226−239

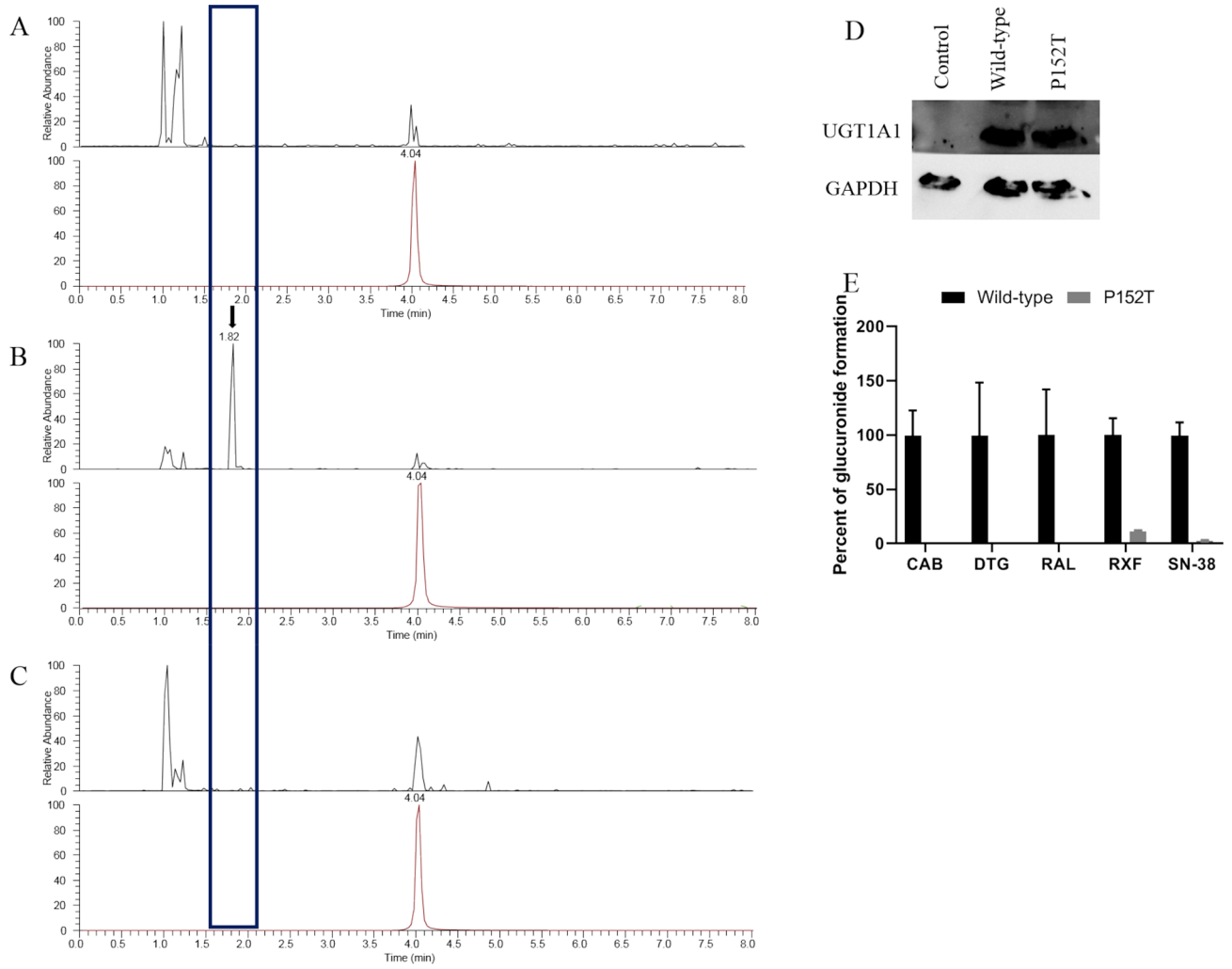

Figure 4. UG1A1 P152T does not exhibit activity toward CAB. Additionally, the glucuronide conjugates of DTG and RAL were not formed in the COS-7 cells expressing the UGT1A1 P152T mutant, whereas the formation of glucuronide conjugates of RXF and SN-38 was reduced in the cells expressing the UGT1A1 P152T mutant. Extracted ion chromatograms of CAB-glucuronide (upper panel; retention time 1.82 min) and CAB (lower panel; retention time 4.04 min) in COS-7 cells that were transfected with (A) no plasmid (control), (B) wild-type UGT1A1 construct, and (C) a mutant construct resulting in expression of UGT1A1 P152T. The arrow indicates the peak corresponding to CAB-glucuronide. All drug treatments were carried out for 24 h. (D) Protein expression of UGT1A1 wild-type and the UGT1A1 P152T mutant in the transfected COS-7 cells. Constructs designed for expression of UGT1A1 wild-type and the UGT1A1 P152T mutant were transfected into COS-7 cells, separately. Transfected COS-7 cells with no plasmid were used as the control. Immunoblot analyses were carried out to detect UGT1A1 expression. (E) Formation of glucuronide conjugates of CAB, DTG, RAL, RXF, and SN-38 in the cells expressing UGT1A1 wild-type versus the UGT1A1 P152T mutant. Error bars represent standard deviation; $n = 3$. Glucuronide formation in the cells expressing UGT1A1 wild-type was normalized to 100%.

toward CAB, DTG, and RAL. In addition, glucuronidation of RXF and SN-38 was reduced in COS-7 cells expressing the UGT1A1 P152T mutant. This observation is in concordance with our in silico prediction of the deleterious impact of the UGT1A1 P152T mutant on activity. In line with this, of the 5 participants carrying the UGT1A1 P152T mutant, 4 (80%, 4/5) individuals did not have detectable levels of CAB-glucuronide following oral administration of CAB. Interestingly, CAB-glucuronide was detected in all participants following intramuscular injection. Future exploration to better understand the pharmacological impact of this variant is warranted.

Of the variants detected in our study, one participant carried a *UGT1A1* variant that involves the substitution of a cystine residue (C510Y). This position (residue 510) is within the C-terminal tail that is highly conserved in UGT enzymes.[30] However, previous studies have shown that substitution of this residue from cystine to a tyrosine does not have a major effect on the activity of UGT1A1 enzyme.[30] In line with this, we did not observe an impact of this variant on CAB glucuronidation. Of note, certain *UGT1A1* variants have been demonstrated to be biologically important. For instance, *UGT1A1* variants such as *UGT1A1*6*, *UGT1A1*28*, and *UGT1A1*37* are associated with Gilbert's syndrome, a condition in which bilirubin processing is impaired.[28,31−33] It is noteworthy that the genotyping of *UGT1A1* has been previously reported in the context of the metabolism of another HIV integrase inhibitor, RAL.[34] The investigators showed that the *UGT1A1*28* polymorphism has a significant impact on RAL exposure with higher RAL plasma levels among *UGT1A1*28* carriers compared to wild-type *UGT1A1*.[34] More recently, the pharmacogenetic effects of the above-mentioned variants (reduced-function alleles, *UGT1A1*6*, *UGT1A1*28*, and *UGT1A1*37*) on steady-state pharmacokinetics and safety of

https://dx.doi.org/10.1021/acsptsci.0c00181
ACS Pharmacol. Transl. Sci. 2021, 4, 226−239

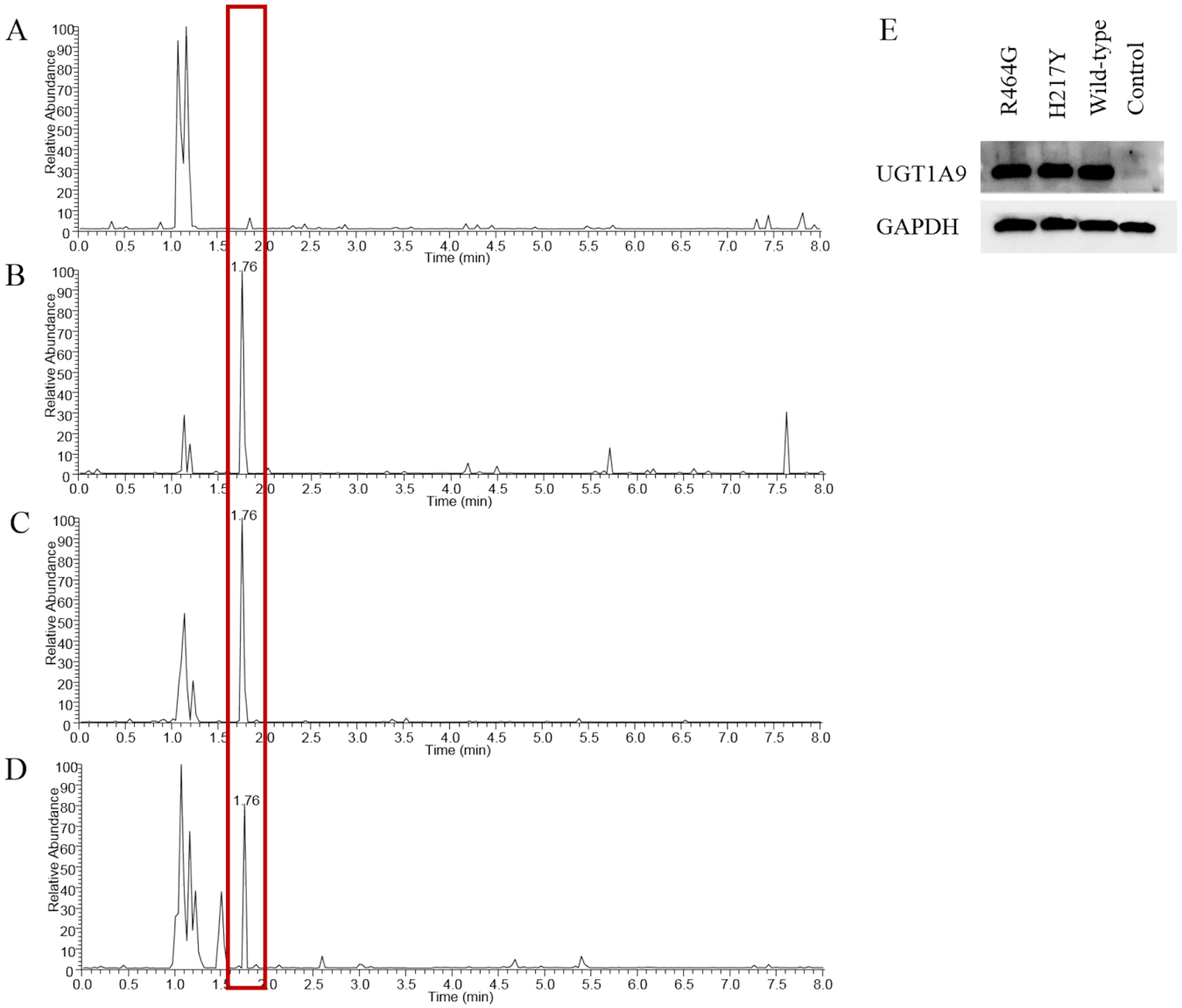

Figure 5. Activity of wild-type UGT1A9, UGT1A9 H217Y, and UGT1A9 R464G toward CAB. Extracted ion chromatograms of CAB-glucuronide (retention time 1.76 min) in COS-7 cells that were transfected with (A) no plasmid (control), (B) wild-type UGT1A9 construct, (C) a variant construct resulting in expression of UGT1A9 H217Y, and (D) a variant construct resulting in expression of UGT1A9 R464G. CAB treatments were carried out for 48 h. While a peak at retention time 1.76 min is visible in panel D, this peak was of low abundance and was not above background. (E) Protein expression of UGT1A9 wild-type, UGT1A9 H217Y, and UGT1A9 R464G in the transfected COS-7 cells. Constructs generated to express UGT1A9 wild-type, UGT1A9 H217Y, and UGT1A9 R464G were transfected into COS-7 cells, separately. Transfected COS-7 cells with no plasmid were used as the control. Immunoblot analyses were carried out to detect UGT1A9 expression.

CAB (both oral and intramuscular injection) have been investigated.[35] This retrospective study showed a modest increase in CAB exposure (following both oral administration and injection) associated with reduced-function alleles though it was not considered clinically relevant.[35] However, we did not detect these reduced-function *UGT1A1* variants (*UGT1A1*6*, *UGT1A1*28*, and *UGT1A1*37*) in our study population.

The *UGT1A9* variant that exhibited the highest frequency (20.6%) in the present work, UGT1A9 H217Y was predicted to be tolerated. Indeed, experiments performed here using cell-based assays confirmed this prediction. The UGT1A9 H217Y mutant is previously unreported and was carried by 14 individuals. Further, two previously reported *UGT1A9* variants detected in our study are predicted to be tolerated: rs750374477 (NM_021027.3:c.850C>T) and rs145084767 (NM_021027.3:c.8G>A). Three participants from two study sites, Chapel Hill/U.S., and Johannesburg/South Africa carried one previously reported *UGT1A9* variant that is predicted to be deleterious, rs200370335 (NM_021027.3:c.1340G>A). The *UGT1A9* genetic variation has been previously suggested to have an impact clinically. For instance, decreased activity of UGT1A9 has been linked to reduced metabolism of a variety of substrates including the active metabolites of the chemotherapeutic agent irinotecan.[36] Further, a *UGT1A9* variant allele, *UGT1A9*3*, has been shown to affect the *in vivo* metabolism of an immunosuppressive drug, mycophenolic acid.[37] In our studies, we found that a UGT1A9 R464G mutant did not produce detectable levels of CAB-glucuronide in cell-based assays. We investigated the cytotoxicity of our study drugs in COS-7 cells and found that the concentrations used in our metabolism assays were near or far below the IC_{50} values for cell viability. These data suggest that drug toxicity

https://dx.doi.org/10.1021/acsptsci.0c00181
ACS Pharmacol. Transl. Sci. 2021, 4, 226−239

likely did not influence our results and confound our ability to effectively compare UGT1A1 and UGT1A9 wild-type to mutant activity.

Specific transporters (both efflux and uptake) involved in the disposition of CAB-glucuronide in humans have been identified.[38] Therefore, the differences in expression of transporters such as multidrug resistance-associated protein 2 (MRP2), MRP3, MRP4, organic anion transporting polypeptide 1B1 (OATP1B1), OATP1B3, and organic anion transporter 3 (OAT3) may contribute to the observed interindividual differences in CAB-glucuronide levels.

In conclusion, we detected 48 previously unreported variants in *UGT1A1* and *UGT1A9*, some of which may impact CAB disposition. Functional testing of UGT1A1 P152T suggests that this mutant may exhibit reduced metabolism of CAB, DTG, RAL, RXF, and SN-38 *in vivo*. Importantly, since this previously unreported variant appears to result in reduced function, it could also impact the glucuronidation of drugs beyond our study drugs. Taken together, these data provide important insights into the genetic variants of *UGT1A1* and *UGT1A9* that may impact the metabolism of CAB as well as other drugs.

AUTHOR INFORMATION

Corresponding Author

Namandjé N. Bumpus − *Department of Pharmacology and Molecular Sciences, The Johns Hopkins University School of Medicine, Baltimore, Maryland 21205, United States*; Phone: +1 410 955 0562; Email: nbumpus1@jhmi.edu

Authors

Herana Kamal Seneviratne − *Department of Medicine, Division of Clinical Pharmacology, The Johns Hopkins University, Baltimore, Maryland 21205, United States*; orcid.org/0000-0002-7221-7060

Allyson N. Hamlin − *Department of Medicine, Division of Clinical Pharmacology, The Johns Hopkins University, Baltimore, Maryland 21205, United States*

Sue Li − *Statistical Center for HIV/AIDS Research and Prevention, Fred Hutchinson Cancer Research Center, Seattle, Washington 98109, United States*

Beatriz Grinsztejn − *Evandro Chagas National Institute of Infectious Diseases, Oswaldo Cruz Foundation, Rio de Janeiro 21040-900, Brazil*

Halima Dawood − *Centre for the AIDS Programme of Research in South Africa, University of KwaZulu Natal, Durban 4041, South Africa*

Albert Y. Liu − *Bridge HIV, Population Health Division, San Francisco Department of Health, San Francisco, California 94102, United States*

Irene Kuo − *Department of Epidemiology and Biostatistics, Milken Institute School of Public Health, George Washington University, Washington, District of Columbia 20052, United States*

Mina C. Hosseinipour − *UNC Project-Malawi, Lilongwe, Malawi*

Ravindre Panchia − *Perinatal HIV Research Unit, Chris Hani Baragwanath Hospital, Soweto 1864, South Africa*

Leslie Cottle − *Statistical Center for HIV/AIDS Research and Prevention, Fred Hutchinson Cancer Research Center, Seattle, Washington 98109, United States*

Gordon Chau − *Statistical Center for HIV/AIDS Research and Prevention, Fred Hutchinson Cancer Research Center, Seattle, Washington 98109, United States*

Adeola Adeyeye − *Division of AIDS, National Institute of Allergy and Infectious Diseases, National Institutes of Health, Rockville, Maryland 20852, United States*

Alex R. Rinehart − *ViiV Healthcare, Durham, North Carolina 27709, United States*

Marybeth McCauley − *FHI360, Durham, North Carolina 27701, United States*

Joseph S. Eron − *University of North Carolina at Chapel Hill, Chapel Hill, North Carolina 27599, United States*

Myron S. Cohen − *University of North Carolina at Chapel Hill, Chapel Hill, North Carolina 27599, United States*

Raphael J. Landovitz − *UCLA, Center for Clinical AIDS Research and Education, Los Angeles, California 90035, United States*

Craig W. Hendrix − *Department of Medicine, Division of Clinical Pharmacology, The Johns Hopkins University, Baltimore, Maryland 21205, United States*

Complete contact information is available at: https://pubs.acs.org/10.1021/acsptsci.0c00181

Author Contributions

H. K. Seneviratne and A. N. Hamlin conducted the experiments, while all of the authors participated in research design and data analysis. The manuscript was written through contributions of all authors. All authors have given approval to the final version of the manuscript.

Notes

The authors declare no competing financial interest.

ACKNOWLEDGMENTS

This work was supported by the HIV Prevention Trials Network (HPTN) sponsored by the National Institute of Allergy and Infectious Diseases (NIAID), National Institute on Drug Abuse, National Institute of Mental Health, and Office of AIDS Research of the NIH, DHHS (Grant UM1 AI068613).

ABBREVIATIONS

CAB, cabotegravir; PrEP, pre-exposure prophylaxis; HPTN, HIV prevention trials network; UGT, uridine diphosphate glucuronosyltransferase; DTG, dolutegravir; RAL, raltegravir; RXF, raloxifene; SN-38, 7-ethyl-10-hydroxycamptothecin

REFERENCES

(1) McPherson, T. D., Sobieszczyk, M. E., and Markowitz, M. (2018) Cabotegravir in the treatment and prevention of Human Immunodeficiency Virus-1. *Expert Opin. Invest. Drugs 27*, 413−420.

(2) Stellbrink, H. J., and Hoffmann, C. (2018) Cabotegravir: its potential for antiretroviral therapy and preexposure prophylaxis. *Curr. Opin. HIV AIDS 13*, 334−340.

(3) Spreen, W. R., Margolis, D. A., and Pottage, J. C. (2013) Long-acting injectable antiretrovirals for HIV treatment and prevention. *Curr. Opin. HIV AIDS 8*, 565−571.

(4) Eisingerich, A. B., Wheelock, A., Gomez, G. B., Garnett, G. P., Dybul, M. R., and Piot, P. K. (2012) Attitudes and acceptance of oral and parenteral HIV preexposure prophylaxis among potential user groups: a multinational study. *PLoS One 7*, No. e28238.

(5) Murray, M. I., Markowitz, M., Frank, I., Grant, R. M., Mayer, K. H., Hudson, K. J., Stancil, B. S., Ford, S. L., Patel, P., Rinehart, A. R., Spreen, W. R., and Margolis, D. A. (2018) Satisfaction and acceptability of cabotegravir long-acting injectable suspension for

prevention of HIV: Patient perspectives from the ECLAIR trial. *HIV Clin. Trials 19*, 129−138.
(6) Spreen, W., Min, S., Ford, S. L., Chen, S., Lou, Y., Bomar, M., St Clair, M., Piscitelli, S., and Fujiwara, T. (2013) Pharmacokinetics, safety, and monotherapy antiviral activity of GSK1265744, an HIV integrase strand transfer inhibitor. *HIV Clin. Trials 14*, 192−203.
(7) Shah, B. M., Schafer, J. J., and Desimone, J. A. (2014) Dolutegravir: a new integrase strand transfer inhibitor for the treatment of HIV. *Pharmacotherapy 34*, 506−520.
(8) Yoshinaga, T., Kobayashi, M., Seki, T., Miki, S., Wakasa-Morimoto, C., Suyama-Kagitani, A., Kawauchi-Miki, S., Taishi, T., Kawasuji, T., Johns, B. A., Underwood, M. R., Garvey, E. P., Sato, A., and Fujiwara, T. (2015) Antiviral characteristics of GSK1265744, an HIV integrase inhibitor dosed orally or by long-acting injection. *Antimicrob. Agents Chemother. 59*, 397−406.
(9) Karmon, S. L., Mohri, H., Spreen, W., and Markowitz, M. (2015) GSK1265744 demonstrates robust in vitro activity against various clades of HIV-1. *JAIDS, J. Acquired Immune Defic. Syndr. 68*, e39−41.
(10) Bowers, G. D., Culp, A., Reese, M. J., Tabolt, G., Moss, L., Piscitelli, S., Huynh, P., Wagner, D., Ford, S. L., Gould, E. P., Pan, R., Lou, Y., Margolis, D. A., and Spreen, W. R. (2016) Disposition and metabolism of cabotegravir: a comparison of biotransformation and excretion between different species and routes of administration in humans. *Xenobiotica 46*, 147−162.
(11) Kobayashi, M., Yoshinaga, T., Seki, T., Wakasa-Morimoto, C., Brown, K. W., Ferris, R., Foster, S. A., Hazen, R. J., Miki, S., Suyama-Kagitani, A., Kawauchi-Miki, S., Taishi, T., Kawasuji, T., Johns, B. A., Underwood, M. R., Garvey, E. P., Sato, A., and Fujiwara, T. (2011) In Vitro antiretroviral properties of S/GSK1349572, a next-generation HIV integrase inhibitor. *Antimicrob. Agents Chemother. 55*, 813−821.
(12) Andrews, C. D., Spreen, W. R., Mohri, H., Moss, L., Ford, S., Gettie, A., Russell-Lodrigue, K., Bohm, R. P., Cheng-Mayer, C., Hong, Z., Markowitz, M., and Ho, D. D. (2014) Long-acting integrase inhibitor protects macaques from intrarectal simian/human immunodeficiency virus. *Science 343*, 1151−1154.
(13) Radzio, J., Spreen, W., Yueh, Y. L., Mitchell, J., Jenkins, L., García-Lerma, J. G., and Heneine, W. (2015) The long-acting integrase inhibitor GSK744 protects macaques from repeated intravaginal SHIV challenge. *Sci. Transl Med. 7*, 270ra5.
(14) Markowitz, M., Frank, I., Grant, R. M., Mayer, K. H., Elion, R., Goldstein, D., Fisher, C., Sobieszczyk, M. E., Gallant, J. E., Van Tieu, H., Weinberg, W., Margolis, D. A., Hudson, K. J., Stancil, B. S., Ford, S. L., Patel, P., Gould, E., Rinehart, A. R., Smith, K. Y., and Spreen, W. R. (2017) Safety and tolerability of long-acting cabotegravir injections in HIV-uninfected men (ECLAIR): a multicentre, double-blind, randomised, placebo-controlled, phase 2a trial. *Lancet HIV 4*, e331−e340.
(15) Landovitz, R. J., Li, S., Grinsztejn, B., Dawood, H., Liu, A. Y., Magnus, M., Hosseinipour, M. C., Panchia, R., Cottle, L., Chau, G., Richardson, P., Marzinke, M. A., Hendrix, C. W., Eshleman, S. H., Zhang, Y., Tolley, E., Sugarman, J., Kofron, R., Adeyeye, A., Burns, D., Rinehart, A. R., Margolis, D., Spreen, W. R., Cohen, M. S., McCauley, M., and Eron, J. J. (2018) Safety, tolerability, and pharmacokinetics of long-acting injectable cabotegravir in low-risk HIV-uninfected individuals: HPTN 077, a phase 2a randomized controlled trial. *PLoS Med. 15*, No. e1002690.
(16) Di, L. (2014) The role of drug metabolizing enzymes in clearance. *Expert Opin. Drug Metab. Toxicol. 10*, 379−393.
(17) Rowland, A., Miners, J. O., and Mackenzie, P. I. (2013) The UDP-glucuronosyltransferases: their role in drug metabolism and detoxification. *Int. J. Biochem. Cell Biol. 45*, 1121−1132.
(18) Yang, G., Ge, S., Singh, R., Basu, S., Shatzer, K., Zen, M., Liu, J., Tu, Y., Zhang, C., Wei, J., Shi, J., Zhu, L., Liu, Z., Wang, Y., Gao, S., and Hu, M. (2017) Glucuronidation: driving factors and their impact on glucuronide disposition. *Drug Metab. Rev. 49*, 105−138.
(19) Liu, S. N., Lu, J. B. L., Watson, C. J. W., Lazarus, P., Desta, Z., and Gufford, B. T. (2019) Mechanistic Assessment of Extrahepatic Contributions to Glucuronidation of Integrase Strand Transfer Inhibitors. *Drug Metab. Dispos. 47*, 535−544.
(20) Margaillan, G., Rouleau, M., Fallon, J. K., Caron, P., Villeneuve, L., Turcotte, V., Smith, P. C., Joy, M. S., and Guillemette, C. (2015) Quantitative profiling of human renal UDP-glucuronosyltransferases and glucuronidation activity: a comparison of normal and tumoral kidney tissues. *Drug Metab. Dispos. 43*, 611−619.
(21) Court, M. H., Zhang, X., Ding, X., Yee, K. K., Hesse, L. M., and Finel, M. (2012) Quantitative distribution of mRNAs encoding the 19 human UDP-glucuronosyltransferase enzymes in 26 adult and 3 fetal tissues. *Xenobiotica 42*, 266−277.
(22) Seneviratne, H. K., Tillotson, J., Lade, J. M., Bekker, L. G., Li, S., Pathak, S., Justman, J., Mgodi, N., Swaminathan, S., Sista, N., Farrior, J., Richardson, P., Hendrix, C. W., and Bumpus, N. N. (2021) Metabolism of Long-Acting Rilpivirine Following Intramuscular Injection: HIV Prevention Trials Network Study 076 (HPTN 076). *AIDS Res. Hum. Retroviruses*, DOI: 10.1089/aid.2020.0155.
(23) Spreen, W., Ford, S. L., Chen, S., Wilfret, D., Margolis, D., Gould, E., and Piscitelli, S. (2014) GSK1265744 pharmacokinetics in plasma and tissue after single-dose long-acting injectable administration in healthy subjects. *JAIDS, J. Acquired Immune Defic. Syndr. 67*, 481−486.
(24) Trezza, C., Ford, S. L., Spreen, W., Pan, R., and Piscitelli, S. (2015) Formulation and pharmacology of long-acting cabotegravir. *Curr. Opin. HIV AIDS 10*, 239−245.
(25) Harbourt, D. E., Fallon, J. K., Ito, S., Baba, T., Ritter, J. K., Glish, G. L., and Smith, P. C. (2012) Quantification of human uridine-diphosphate glucuronosyl transferase 1A isoforms in liver, intestine, and kidney using nanobore liquid chromatography-tandem mass spectrometry. *Anal. Chem. 84*, 98−105.
(26) Gill, K. L., Houston, J. B., and Galetin, A. (2012) Characterization of in vitro glucuronidation clearance of a range of drugs in human kidney microsomes: comparison with liver and intestinal glucuronidation and impact of albumin. *Drug Metab. Dispos. 40*, 825−835.
(27) Ciotti, M., Cho, J. W., George, J., and Owens, I. S. (1998) Required buried alpha-helical structure in the bilirubin UDP-glucuronosyltransferase, UGT1A1, contains a nonreplaceable phenylalanine. *Biochemistry 37*, 11018−11025.
(28) Yamamoto, K., Sato, H., Fujiyama, Y., Doida, Y., and Bamba, T. (1998) Contribution of two missense mutations (G71R and Y486D) of the bilirubin UDP glycosyltransferase (UGT1A1) gene to phenotypes of Gilbert's syndrome and Crigler-Najjar syndrome type II. *Biochim. Biophys. Acta, Mol. Basis Dis. 1406*, 267−273.
(29) Takeuchi, K., Kobayashi, Y., Tamaki, S., Ishihara, T., Maruo, Y., Araki, J., Mifuji, R., Itani, T., Kuroda, M., Sato, H., Kaito, M., and Adachi, Y. (2004) Genetic polymorphisms of bilirubin uridine diphosphate-glucuronosyltransferase gene in Japanese patients with Crigler-Najjar syndrome or Gilbert's syndrome as well as in healthy Japanese subjects. *J. Gastroenterol. Hepatol. 19*, 1023−1028.
(30) Ghosh, S. S., Lu, Y., Lee, S. W., Wang, X., Guha, C., Roy-Chowdhury, J., and Roy-Chowdhury, N. (2005) Role of cysteine residues in the function of human UDP glucuronosyltransferase isoform 1A1 (UGT1A1). *Biochem. J. 392*, 685−692.
(31) Bosma, P. J., Chowdhury, J. R., Bakker, C., Gantla, S., de Boer, A., Oostra, B. A., Lindhout, D., Tytgat, G. N.J., Jansen, P. L.M., Elferink, R. P.J. O., and Chowdhury, N. R. (1995) The genetic basis of the reduced expression of bilirubin UDP-glucuronosyltransferase 1 in Gilbert's syndrome. *N. Engl. J. Med. 333*, 1171−1175.
(32) Mackenzie, P. I., Owens, I. S., Burchell, B., Bock, K W, Bairoch, A., Belanger, A., Gigleux, S. F., Green, M., Hum, D. W., Iyanagi, T., Lancet, D., Louisot, P., Magdalou, J., Roy Chowdhury, J., Ritter, J. K., Tephly, T. R., Schachter, H., Tephly, T., Tipton, K. F, and Nebert, D. W. (1997) The UDP glycosyltransferase gene superfamily: recommended nomenclature update based on evolutionary divergence. *Pharmacogenetics 7*, 255−269.
(33) Beutler, E., Gelbart, T., and Demina, A. (1998) Racial variability in the UDP-glucuronosyltransferase 1 (UGT1A1) promoter: a balanced polymorphism for regulation of bilirubin metabolism? *Proc. Natl. Acad. Sci. U. S. A. 95*, 8170−8174.

(34) Belkhir, L., Seguin-Devaux, C., Elens, L., Pauly, C., Gengler, N., Schneider, S., Ruelle, J., Haufroid, V., and Vandercam, B. (2018) Impact of UGT1A1 polymorphisms on Raltegravir and its glucuronide plasma concentrations in a cohort of HIV-1 infected patients. *Sci. Rep. 8*, 7359.
(35) Patel, P., Xue, Z., King, K. S., Parham, L., Ford, S., Lou, Y., Bakshi, K. K., Sutton, K., Margolis, D., Hughes, A. R., and Spreen, W. R. (2020) Evaluation of the effect of UGT1A1 polymorphisms on the pharmacokinetics of oral and long-acting injectable cabotegravir. *J. Antimicrob. Chemother.*, DOI: 10.1093/jac/dkaa147.
(36) Olson, K. C., Dellinger, R. W., Zhong, Q., Sun, D., Amin, S., Spratt, T. E., and Lazarus, P. (2009) Functional characterization of low-prevalence missense polymorphisms in the UDP-glucuronosyltransferase 1A9 gene. *Drug Metab. Dispos. 37*, 1999−2007.
(37) Bernard, O., and Guillemette, C. (2004) The main role of UGT1A9 in the hepatic metabolism of mycophenolic acid and the effects of naturally occurring variants. *Drug Metab. Dispos. 32*, 775−778.
(38) Patel, M., Eberl, H. C., Wolf, A., Pierre, E., Polli, J. W., and Zamek-Gliszczynski, M. J. (2019) Mechanistic Basis of Cabotegravir-Glucuronide Disposition in Humans. *J. Pharmacol. Exp. Ther. 370*, 269−277.

https://dx.doi.org/10.1021/acsptsci.0c00181
ACS Pharmacol. Transl. Sci. 2021, 4, 226−239